

Switching Differentiator

Jang-Hyun Park

Abstract—A novel switching differentiator that has considerably simple form is proposed. Under the assumption that time-derivatives of the signal are norm-bounded, it is shown that estimation errors are convergent to the zeros asymptotically. The estimated derivatives shows neither chattering nor peaking phenomenon. A 1st-order differentiator is firstly proposed and, by connecting this differentiator in series, higher-order derivatives are also available. Simulation results show that the proposed differentiator show extreme performance compared to the widely used previous differentiators such as high-gain observer or high-order sliding mode differentiator.

Index Terms—switching differentiator, time-derivative estimator, state observer.

I. INTRODUCTION

On-line differentiator for a given signal is widely utilized in control system containing PID regulators [1], states observers [2], [3], [4], [5], [6], fault diagnosis schemes [7], and active disturbance rejection [8], [1]. The performance of the differentiator is crucial since it is directly connected to that of the controller. To mention just a few, there are linear differentiator [9], high-gain observer (HGO) [2], [3], high-order sliding mode (HOSM) differentiator [5], [6], the super-twisting second-order sliding-mode algorithm [10], uniformly convergent differentiator [11], singular perturbation technique based differentiator [12], augmented nonlinear differentiator (AND) [13], etc.

Among the various differentiators, HGO and HOSM differentiator are widely adopted in the controller design for nonlinear systems. The HGO whose dynamics is linear in the estimation error has a shortcoming of peaking due to nonzero initial condition. This also leads to the non-robust against measurement disturbance. The HOSM differentiator has the property of finite-time exact convergence. However, since it contains discontinuous switching function in its dynamics, the chattering in its estimations are inevitable and its dynamics are rather complex. In the presented differentiators in [10], [12], [11], [13], their nonlinear dynamics become complicated which leads to numerical problems for the practical use as well as simulation come out.

In this paper, a novel switching differentiator (SD) that has considerably simple form is proposed. Under the assumption that time-derivative of the signal is norm-bounded, it is proven that estimation error is asymptotically convergent to the zero. The observed derivative shows neither chattering nor peaking phenomenon. A 1st-order derivative estimator is firstly proposed and, by connecting the proposed differentiators in series, it is shown that higher-order derivatives are also available. Simulation results depict that the proposed differentiator shows

extreme performance compared to other well-known differentiators.

II. MAIN RESULT

A. Switching Differentiator

Consider the time-varying signal $a(t)$ whose time derivative is to be estimated. Assume that $|\ddot{a}(t)| \leq L^*$ holds $\forall t > 0$. The proposed SD has the following form

$$\begin{aligned}\dot{\alpha} &= ke_\alpha + \sigma \\ \dot{\sigma} &= L \operatorname{sgn}(e_\alpha).\end{aligned}\quad (1)$$

where $e_\alpha = a - \alpha$, k is a positive design constant and L is determined such that $L > L^*$. The α and σ are expected to estimate a and \dot{a} respectively. The second error is denoted as

$$e_\sigma = \dot{a} - \sigma \quad (2)$$

and whether this e_σ will converge to zero as time goes by is a main concern. Our main result is in the following theorem.

Theorem 1: The $\sigma(t)$ in (1) is asymptotically convergent to $\dot{a}(t)$.

proof. The time-derivatives of e_α and e_σ are derived as

$$\dot{e}_\alpha = -ke_\alpha + e_\sigma \quad (3)$$

$$\dot{e}_\sigma = \ddot{a} - L \operatorname{sgn}(e_\alpha). \quad (4)$$

It is assumed the worst cast that the signal $\ddot{a}(t)$ acts to hinder the estimation as much as possible. This means that when $e_\alpha(t) > 0$, $\ddot{a}(t)$ maintains its extreme value L^* which reduces the switching gain utmost. Conversely, if $e_\alpha(t)$ is negative then $\ddot{a}(t)$ is assumed to maintain $-L^*$. Considering this assumption, (4) can be redescribed as

$$\dot{e}_\sigma = -L_\delta \operatorname{sgn}(e_\alpha) \triangleq r(t) \quad (5)$$

where $L_\delta = L - L^* (> 0)$. From (3) and (5), the following dynamics is induced

$$\begin{aligned}\ddot{e}_\alpha &= -k\dot{e}_\alpha + \dot{e}_\sigma \\ &= -k\dot{e}_\alpha + r(t).\end{aligned}\quad (6)$$

Defining $e_\alpha^d \triangleq \dot{e}_\alpha$, (6) becomes

$$\dot{e}_\alpha^d = -ke_\alpha^d + r(t) \quad (7)$$

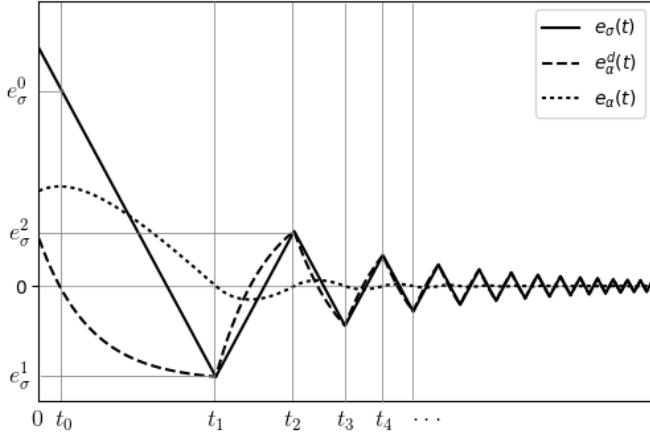
whose solution is

$$e_\alpha^d(t) = e_\alpha^d(0)e^{-kt} + \int_0^t r(\tau)e^{-k(t-\tau)}d\tau. \quad (8)$$

In the case that $e_\alpha(t) > 0$ holds for $0 \leq t < t_1$, the solution for $e_\alpha^d(t)$ is

$$e_\alpha^d(t) = e_\alpha^d(0)e^{-kt} - L_\delta \int_0^t e^{-k(t-\tau)}d\tau$$

J.-H. Park is with the Department of Electrical and Control Engineering, Mokpo National University, Chonnam 58554, Korea (e-mail: jh-park72@mokpo.ac.kr)


 Fig. 1. Typical trajectory of $e_\sigma(t)$, $e_\sigma^d(t)$ and $e_\alpha(t)$.

$$\begin{aligned} &= e_\alpha^d(0)e^{-kt} - \frac{L_\delta}{k}(1 - e^{-kt}) \\ &= (e_\alpha^d(0) + \rho)e^{-kt} - \rho \end{aligned} \quad (9)$$

since $r(t) = -L_\delta$ for $t < t_1$ where $\rho = \frac{L_\delta}{k}$. Because the first term decays exponentially, it is evident that there is $t_0 (< t_1)$ such that $e_\alpha^d(t)$ become negative for $t > t_0$. In the other case that the initial error $e_\alpha(0)$ is negative, similar explanation is possible since $r(t) = L_\delta$ and

$$e_\alpha^d(t) = (e_\alpha^d(0) - \rho)e^{-kt} + \rho \quad (10)$$

Note that the t_0 can be made arbitrarily small by increasing ρ . In either cases, there exist t_0 and t_1 ($0 < t_0 < t_1$) such that $e_\alpha(t)$ turns its direction toward zero at $t = t_0$ and becomes zero at $t = t_1$. The typical trajectories of $e_\sigma(t)$, $e_\alpha^d(t)$ and $e_\alpha(t)$ are illustrated in fig. 1 for the convenience of the proof follows.

Let the time points that $e_\alpha(t) = 0$ holds be denoted as t_i , ($i = 1, 2, \dots$). It is evident from (3) that $e_\alpha(t_i) = 0$ if and only if $e_\alpha^d(t_i) = e_\sigma(t_i)$. Since, in the time interval $t_i < t \leq t_{i+1}$, $r(t)$ is constant (either $-L_\delta$ or L_δ), the time solutions of $e_\alpha^d(t)$ and $e_\sigma(t)$ for $t_i < t \leq t_{i+1}$ are

$$e_\alpha^d(t) = e_\sigma(t_i)e^{-k(t-t_i)} + \frac{r}{k}(1 - e^{-k(t-t_i)}) \quad (11)$$

$$e_\sigma(t) = e_\sigma(t_i) + r(t-t_i). \quad (12)$$

Here, $e_\alpha^d(t_i) = ke_\alpha(t_i) + e_\sigma(t_i) = e_\sigma(t_i)$ holds due to $e_\alpha(t_i) = 0$. The two right-hand sides of (11) and (12) must be identical at $t = t_{i+1}$. Denoting $t_\delta^i \triangleq t_{i+1} - t_i$ and $e_\sigma^i = e_\sigma(t_i)$ yields

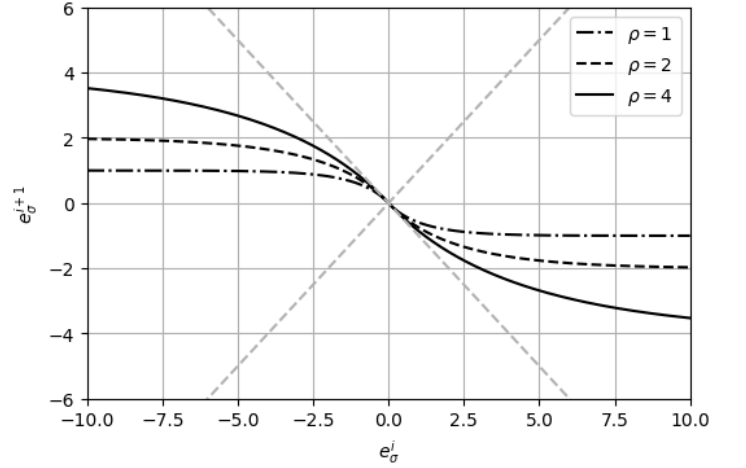
$$e_\sigma^i e^{-kt_\delta^i} + \frac{r}{k}(1 - e^{-kt_\delta^i}) = e_\sigma^i + rt_\delta^i \quad (13)$$

or

$$\left(e_\sigma^i - \frac{r}{k}\right) + rt_\delta^i = \left(e_\sigma^i - \frac{r}{k}\right) e^{-kt_\delta^i} \quad (14)$$

Note that the solution of $A + Bt = De^{-Ct}$ is $t = \frac{1}{C}W\left[\frac{CD}{B}e^{\frac{AC}{B}}\right] - \frac{A}{B}$ where $W(\cdot)$ is Lambert-W function. Using this formula with

$$\begin{aligned} A &= D = \left(e_\sigma^i - \frac{r}{k}\right) \\ B &= r \\ C &= k \end{aligned} \quad (15)$$


 Fig. 2. The graphs of e_σ^{i+1} versus e_σ^i with different ρ 's and $e_\sigma^{i+1} = \pm e_\sigma^i$ lines.

and defining

$$\begin{aligned} x &\triangleq \frac{CD}{B} = \frac{AC}{B} \\ &= \frac{k}{r}e_\sigma^i - 1 = -\frac{k}{L_\delta}|e_\sigma^i| - 1 \\ &= -\frac{|e_\sigma^i|}{\rho} - 1 < -1 \end{aligned} \quad (16)$$

the solution of (14) is

$$t_\delta^i = -\frac{e_\sigma^i}{r} + \frac{1}{k}(1 + W(xe^x)) \quad (17)$$

Using this time interval, $e_\sigma^{i+1} := e_\sigma(t_{i+1})$ which is the function of e_σ^i can be obtained from (5) as

$$\begin{aligned} e_\sigma^{i+1} &= e_\sigma^i + \int_{t_i}^{t_{i+1}} r dt \\ &= e_\sigma^i + rt_\delta^i \\ &= \frac{r}{k}(1 + W(xe^x)) \end{aligned} \quad (18)$$

or

$$e_\sigma^{i+1} = -\text{sgn}(e_\sigma^i)\rho(1 + W(xe^x)). \quad (19)$$

The value of $W(xe^x)$ is -1 at $x = -1$ and approaches to 0^- as x goes to $-\infty$. The graphs of e_σ^{i+1} versus e_σ^i with different ρ 's are illustrated in fig. 2. The slope of e_σ^{i+1} curve at $e_\sigma^i = 0$, which is denoted as z in what follows, can be calculated from (18) as

$$\begin{aligned} z &\triangleq \frac{de_\sigma^{i+1}}{de_\sigma^i} \Big|_{e_\sigma^i=0} = \frac{r}{k} \frac{dW(xe^x)}{de_\sigma^i} \Big|_{e_\sigma^i=0} \\ &= \frac{r}{k} \frac{e^x W(xe^x)}{xe^x} \Big|_{e_\sigma^i=0} \frac{e_\sigma^i}{1 + W(xe^x)} \Big|_{e_\sigma^i=0} \\ &= \frac{r}{k} \frac{e_\sigma^i}{1 + W(xe^x)} \Big|_{e_\sigma^i=0} \end{aligned} \quad (20)$$

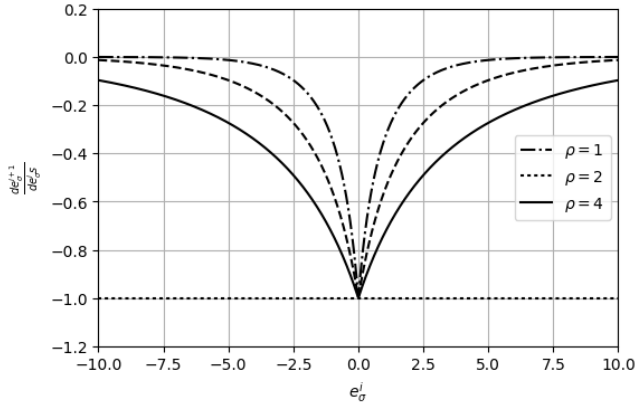


Fig. 3. The graphs of $\frac{de_{\sigma}^{i+1}}{de_{\sigma}^i}$ with different ρ 's.

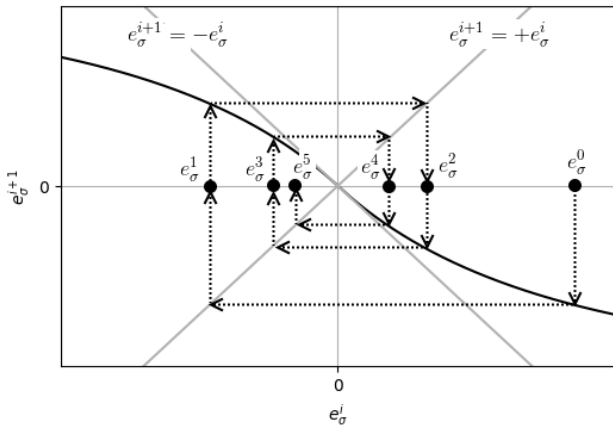


Fig. 4. Typical variations of e_{σ}^i 's by (18) for $i = 0, 1, 2, 3, 4, 5$. (black dots in e_{σ}^i axis)

since $x(e_{\sigma}^i = 0) = -1$ and $W(-e^{-1}) = -1$. The numerator and denominator of the last term are all zeros. Thus, applying L'Hopital's theorem and deriving w.r.t e_{σ}^i both of them yields

$$\begin{aligned} z &= \frac{r}{k} \frac{1}{\left. \frac{de_{\sigma}^{i+1}}{de_{\sigma}^i} \right|_{e_{\sigma}^i=0}} = \frac{r}{k} \frac{1}{\frac{k}{r} z} \\ &= \frac{1}{z} \end{aligned} \quad (21)$$

where we used (20). It is evident from $z < 0$ (refer to fig. 2) that the valid solution of z is -1 . The graphs are illustrated in fig. 3 for some ρ 's. This means that the e_{σ}^{i+1} curve is exactly tangent to the $e_{\sigma}^{i+1} = -e_{\sigma}^i$ line at the origin and there are no crossing points between them except the origin. Thus, this results in asymptotical convergence of $|e_{\sigma}^i|$ to zero because $|e_{\sigma}^{i+1}| < |e_{\sigma}^i|$ for all $i > 0$. The typical variations of e_{σ}^i 's are illustrated in fig.4 as a black dot in e_{σ}^i axis. This completes the proof.

Note that the convergence properties hold globally and uniformly, which means that the errors converge to the zeros regardless of large initial gaps. The initial values of α and σ can usually be chosen as zeros since the informations on $a(0)$ and $\dot{a}(0)$ may be difficult to obtain *a priori* in practice. It is worth noting that the proposed SD shows no peaking

phenomenon caused by nonzero initial errors during transient period. This property is very crucial because it leads to the robustness against measurement noise.

It is also worth noting that the effect of the discontinuous switching function $\text{sgn}(e_{\alpha})$ is integrated and, therefore, the chattering in σ is suppressed. In practice, it is hard to obtain the bounds on the norm-bound of $\ddot{a}(t)$, which leads to choose L as a sufficiently large value. This is admissible since the chattering is suppressed by this reason, and it will be shown in simulations later.

B. Higher-Order Differentiator

The higher-order time derivatives of $a(t)$ can be available via series connection of (1). The series equations for $i = 1, 2, \dots$ are

$$\begin{aligned} \dot{\alpha}_i &= ke_{\alpha i} + \sigma_i \\ \dot{\sigma}_i &= L \text{sgn}(e_{\alpha i}) \end{aligned} \quad (22)$$

where $e_{\alpha i} = \sigma_{i-1} - \alpha_i$ with $\sigma_0 = a(t)$. The L is determined sufficiently large such that $L > \max_i L_i^*$ where $|a^{i+1}(t)| \leq L_i^*$. Then, the estimate of $a^{(i)}(t)$ is $\sigma_i(t)$ which is also expected to be asymptotically convergent.

III. SIMULATIONS

In this section, using the proposed SD and other well-known differentiators, the time derivatives $\dot{a}(t)$ up to $a^{(4)}(t)$ are estimated through simulations where of $a(t) = 2 \sin t + 3 \cos 3t$. To compare the performances with each other, the settling time of the estimate of $a^{(4)}$ is deliberately set to about 0.1s via tuning their design parameters.

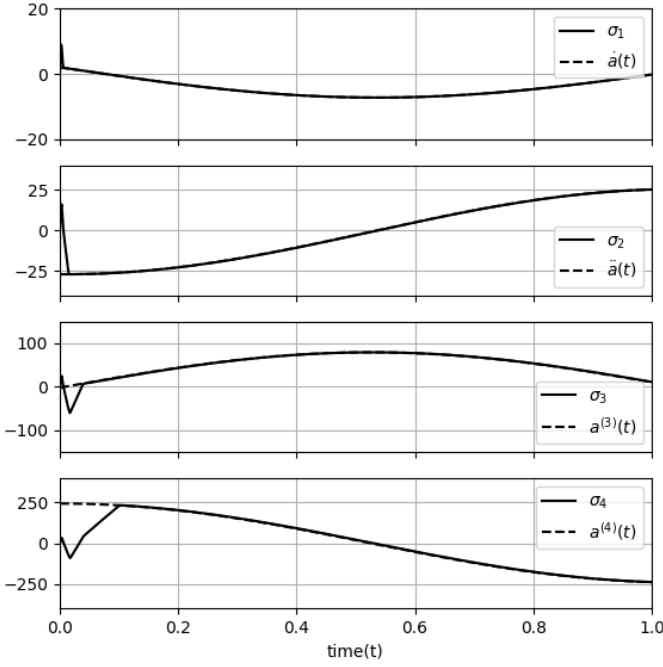
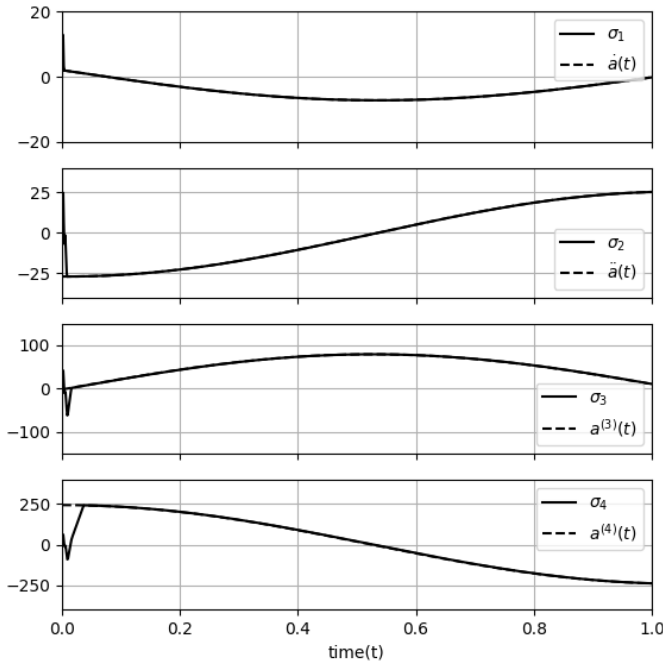
A. Proposed SD

The proposed series SDs (22) is used to observe \dot{a} , \ddot{a} , \dddot{a} and $a^{(4)}$. The whole formulas whose dynamic order is 8 is as follows.

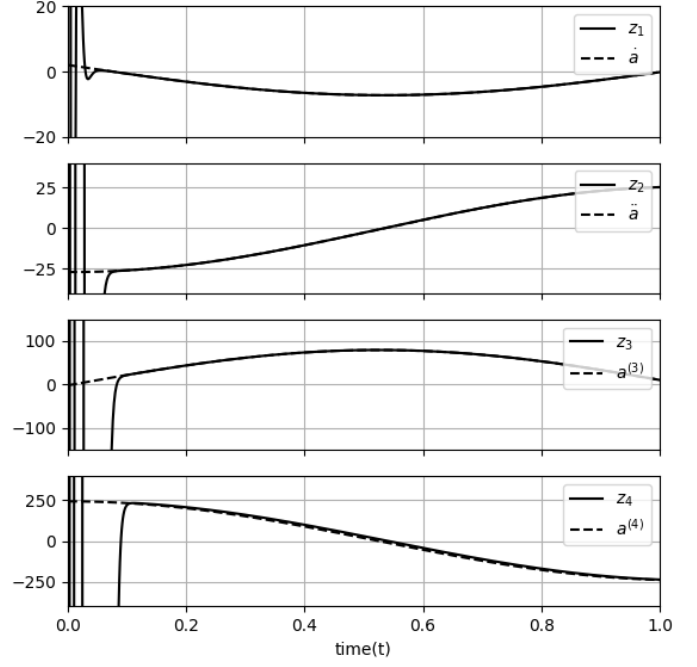
$$\begin{aligned} \dot{\alpha}_1 &= ke_{\alpha 1} + \sigma_1 \quad \text{with } e_{\alpha 1} = a(t) - \alpha_1 \\ \dot{\sigma}_1 &= L \text{sgn}(e_{\alpha 1}) \\ \dot{\alpha}_2 &= ke_{\alpha 2} + \sigma_2 \quad \text{with } e_{\alpha 2} = \sigma_1 - \alpha_2 \\ \dot{\sigma}_2 &= L \text{sgn}(e_{\alpha 2}) \\ \dot{\alpha}_3 &= ke_{\alpha 3} + \sigma_3 \quad \text{with } e_{\alpha 3} = \sigma_2 - \alpha_3 \\ \dot{\sigma}_3 &= L \text{sgn}(e_{\alpha 3}) \\ \dot{\alpha}_4 &= ke_{\alpha 4} + \sigma_4 \quad \text{with } e_{\alpha 4} = \sigma_3 - \alpha_4 \\ \dot{\sigma}_4 &= L \text{sgn}(e_{\alpha 4}) \end{aligned} \quad (23)$$

The estimation of $a^{(i)}$ is σ_i for $i = 1, 2, 3, 4$. The parameters are chosen as $k = 3000$, $L = 3000$. For the simulations, we used $\text{sat}(\frac{e_{\alpha i}}{\epsilon})$ with $\epsilon = 10^{-4}$ instead of $\text{sgn}(e_{\alpha i})$ for $i = 1, 2, 3, 4$. Initial values of all the states in SDs are set to zeros. The result is in Fig. 5. Even in $\sigma_4(t)$ which is the estimation of $a^{(4)}(t)$ follows exactly to the real value after transient time of 0.1 sec without any peaking or chattering.

Note that the transient time can be shortened further through increasing k and L . In fig. 6, the simulation result is shown with parameters $k = 5000$, $L = 10000$. The settling time is shortened compared to fig. 5. It is worth to note that, in


 Fig. 5. estimates of $\dot{a}(t)$, $\ddot{a}(t)$, $\dddot{a}(t)$, and $a^{(4)}(t)$ using proposed SSDs.

 Fig. 6. estimates of $\dot{a}(t)$, $\ddot{a}(t)$, $\dddot{a}(t)$, and $a^{(4)}(t)$ using proposed SSDs.

determining L , the upper bound of $a^{(5)}$ is not considered and it is chosen as sufficiently large value. For fairly large values of k and L , the proposed SDs show extreme performance while generating no peaking nor chattering in the estimated values at least in the simulations.


 Fig. 7. estimates of $\dot{a}(t)$, $\ddot{a}(t)$, $\dddot{a}(t)$, and $a^{(4)}(t)$ using HGO.

B. HGO

The derivatives of the same signal using HGO [2] that has the following dynamics are estimated.

$$\begin{aligned}\dot{z}_0 &= z_1 + (c_0/\epsilon)(a - z_0) \\ \dot{z}_1 &= z_2 + (c_1/\epsilon^2)(a - z_0) \\ \dot{z}_2 &= z_3 + (c_2/\epsilon^3)(a - z_0) \\ \dot{z}_3 &= z_4 + (c_3/\epsilon^4)(a - z_0) \\ \dot{z}_4 &= (c_4/\epsilon^5)(a - z_0)\end{aligned}\quad (24)$$

where z_i ($i = 1, 2, 3, 4$) is the estimates of $a^{(i)}$. The parameters are determined such that the settling time of z_4 is about 0.1s as before. The determined parameters are $c_0 = 47.5$, $c_1 = 902.5$, $c_2 = 8573.75$, $c_3 = 40725.3125$, $c_4 = 77378.09375$ and $\epsilon = 0.03$. The result is illustrated in Fig. 7. In this figure, the y-axis limits are identical to those of fig. 5 for the convenience of comparison. Note that the peaking in transient period is enormous and grow rapidly as i increases. In this simulation, the peak value for z_1 is 1552.1 and about 4×10^9 for z_4 .

C. HOSM differentiator

The HOSM differentiator [5] for estimating up to $a^{(4)}$ has the following form.

$$\begin{aligned}\dot{z}_0 &= -8L^{\frac{1}{5}}[z_0 - a]^{\frac{4}{5}} \triangleq v_0 \\ \dot{z}_1 &= -5L^{\frac{1}{4}}[z_1 - v_0]^{\frac{3}{4}} \triangleq v_1 \\ \dot{z}_2 &= -3L^{\frac{1}{3}}[z_2 - v_1]^{\frac{2}{3}} \triangleq v_2 \\ \dot{z}_3 &= -1.5L^{\frac{1}{2}}[z_3 - v_2]^{\frac{1}{2}} \triangleq v_3 \\ \dot{z}_4 &= -1.1L \operatorname{sgn}(z_4 - v_3)\end{aligned}\quad (25)$$

where $[z]^p = |x|^p \operatorname{sgn}(x)$ and L is a positive design constant. The estimate of $a^{(i)}$ is z_i . It is hard to satisfy the condition that the settling time of z_4 is 0.1s without using fairly large L value. Thus, we has chosen $L = 3 \times 10^7$, which leads to severe chattering in z_4 as shown in fig. 8.

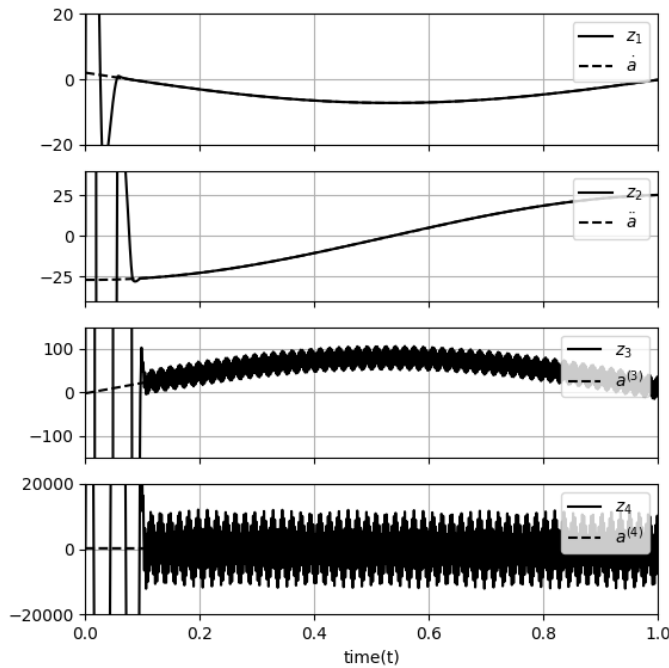


Fig. 8. estimates of $\dot{a}(t)$, $\ddot{a}(t)$, $\dddot{a}(t)$, and $a^{(4)}(t)$ using HOSM differentiator.

IV. CONCLUSION

A novel SD that has considerably simple dynamics is proposed. Under the assumption that time-derivatives of the signal are norm-bounded, it is shown that estimation error is convergent to the zeros asymptotically. The estimated derivative shows neither chattering nor peaking phenomenon and tracks the desired value exactly after finite transient period. A 1st-order differentiator is firstly proposed and, by connecting this differentiator in series, higher-order derivatives are also available. Simulation results depict that the proposed differentiators show extreme performances compared to the widely used previous differentiators such as HGO or HOSM differentiator.

REFERENCES

- [1] J. Han, "From pid to active disturbance control," *IEEE Trans. Industrial Electronics*, vol. 56, no. 3, pp. 900–906, 2009.
- [2] H. K. Khalil, "High-gain observers in feedback control," *IEEE Control Systems Magazine*, pp. 25–41, June, 2017.
- [3] —, "Cascade high-gain observers in output feedback control," *Automatica*, vol. 80, pp. 110–118, 2017.
- [4] A. E. Bryson and Y. C. Ho, *Applied Optimal Control*. New York:Blaisdell, 1969.
- [5] A. Levant, "Higher-order sliding modes, differentiation and output-feedback control," *Int. J. Control*, vol. 76, no. 9/10, pp. 924–941, 2003.
- [6] —, "Non-homogeneous finite-time-convergent differentiator," *proceedings of the 48th IEEE conference on decision and control*, pp. 8399–8404, 2009.
- [7] D. Efimov, A. Zolghadri, T. Raissi, "Actuator fault detection and compensation under feedback control," *Automatica*, vol. 47, no. 8, pp. 1699–1705, 2011.
- [8] Z. Gao, "Active disturbance rejection control:a paradigm shift in feedback control design," *Proceedings of the 2006 American Control Conference*, June 15,2006.
- [9] S.-C. Pei, J.-J. Shyu, "Design of fir hilbert transformers and differentiators by eigenfilter," *IEEE Trans. Acoust., Speech, Signal Process.*, vol. 37, pp. 505–511, 1989.
- [10] J. Davila, L. Fridman, A. Levant, "Second-order sliding-modes observer for mechanical systems," *IEEE Trans. Automatic Control*, vol. 50, no. 11, pp. 1785–1789, 2005.

- [11] M. T. Angulo, J. A. Moreno, L. Fridman, "Robust exact uniformly convergent arbitrary order differentiator," *Automatica*, vol. 49, pp. 2489–2495, 2013.
- [12] X. Wang, Z. Chen, G. Yang, "Finite-time-convergent differentiator based on singular perturbation technique," *IEEE Trans. Automatic Control*, vol. 52, no. 9, pp. 1731–1737, 2007.
- [13] X. Shao, et. al., "Augmented nonlinear differentiator design and application to nonlinear uncertain systems," *ISA Transactions*, vol. 67, pp. 30–46, 2017.